Synthesis and VUV Photoluminescence Characterization of $(Y,Gd)(V,P)O_4:Eu^{3+}$ as a Potential Red-emitting PDP Phosphor

Chia-Chin Wu,[†,‡] Kuei-Bo Chen,[§] Chi-Sen Lee,[§] Teng-Ming Chen,*[,†] and Bing-Ming Cheng[#]

Phosphor Research Laboratory and Applied Solid-State Laboratory, Department of Applied Chemistry, National Chiao Tung University, Hsinchu 30010, Taiwan, Materials and Chemical Research Laboratories, Industrial Technology Research Institute, Hsinchu, 30040 Taiwan, and National Synchrotron Radiation Research Center, Hsinchu Science Park, Hsinchu 30076, Taiwan

Received May 5, 2006. Revised Manuscript Received March 6, 2007

$YVO_4:Eu^{3+}$-based phosphors in three series with compositions $(Y_{1-x}Eu_x)(V_{1-z}P_z)O_4$, $(Y_{0.95-y}Gd_yEu_{0.05})(V_{0.4}P_{0.6})O_4$ and $(Y_{0.95-y}Eu_{0.05}Gd_y)(V_{1-z}P_z)O_4$ were synthesized and investigated as potential red-emitting phosphors for a plasma display panel (PDP). The optimal substitution proportions of P for V and Gd for Y were determined to be 60 and 20 mol %, respectively, for $(Y_{0.95-y}Gd_y)(V_{1-z}P_z)O_4$ doped with 5 mol % Eu^{3+}. The vacuum ultraviolet PL and PLE spectra and chromaticity characteristics for the synthesized phosphors were measured and compared against those of a commercial red-emitting phosphor. Pumping the $(Y,Gd)(P,V)O_4:Eu^{3+}$ phosphors at a wavelength of 172 nm is more efficient than that at 147 nm. For VUV excitation at 147 nm, the CIE chromaticity coordinates for our red-emitting $(Y_{1-y}Gd_y)(V_{0.4}P_{0.6})O_4:Eu^{3+}$ are (0.6614,0.3286), as compared to (0.6443, 0.3613) for $(Y,Gd)BO_3:Eu^{3+}$ from Kasei Optonix Ltd. We suggest that the composition-optimized $(Y_{0.75}Gd_{0.20}Eu_{0.05})(V_{0.4}P_{0.6})O_4$ can serve as an alternative phosphor to replace a widely used red-emitting commercial phosphor such as $(Y,Gd)BO_3:Eu^{3+}$ or $Y_2O_3:Eu^{3+}$.

1. Introduction

A plasma display panel (PDP) has become regarded as a promising candidate for a display with a large area mainly because its emissive features include a wide viewing angle and high brightness. PDP phosphors are expected to meet the critical requirements to yield a high luminous efficiency on excitation with vacuum ultraviolet (VUV) radiation of wavelengths 147 and 172 nm generated from a plasma of a mixture of He and Xe noble gases. To improve the performance of PDP, we investigated the development of efficient VUV-excitable phosphors. Oxide phosphors with aluminate, silicate, vanadate, phosphate, and borate groups generally exhibit strong absorption in the VUV spectral region.[1−3] The main weaknesses of commercial phosphors in current use are the lack of color purity of a red-emitting phosphor such as $(Y,Gd)BO_3:Eu^{3+}$, a long decay lifetime of green-emitting phosphors such as $Zn_2SiO_4:Mn^{2+}$ and $BaAl_{12}O_{19}:Mn^{2+}$, and color degradation attributed to material instability of a blue-emitting phosphor such as $BaMgAl_{10}O_{17}:Eu^{2+}$. For these reasons, the optical and luminescence properties such as luminous efficiency, purity of chromaticity and saturation, and decay lifetime of PDP phosphors have been widely investigated.[4−6]

Being considered as a red-emitting phosphor, $(Y,Gd)BO_3:Eu^{3+}$ is well-known as a PDP phosphor because of its high luminous efficiency under VUV excitation at 147 nm. However, its main emission appearing at 593 nm and attributed to Eu^{3+} yields poor and unsaturated red color chromaticity. The red emission attributed to the transition $^5D_0 \rightarrow {}^7F_2$ of Eu^{3+} is hypersensitive to the lattice symmetry of the host matrix, and its luminescent intensity is expected to be strong if the symmetry of the crystal is lowered.[7] The Eu^{3+} ion occupies a lattice site with inversion symmetry in $(Y,Gd)BO_3:Eu^{3+}$; the transition $^5D_0 \rightarrow {}^7F_1$ (593 nm) thus predominates.[8] Furthermore, the well-known phosphor Eu^{3+}-activated $Y(P,V)O_4$ used for high-pressure mercury lamps has been reinvestigated and evaluated as an alternative phosphor for PDP application as it exhibits a greater color saturation in the red with color coordinates (0.66, 0.33) than that with coordinates (0.65, 0.36) of conventional $(Y,Gd)BO_3:Eu^{3+}$.[9] A quest for red-emitting PDP phosphors with improved efficiency, brightness, and color saturation has

* To whom correspondence should be addressed. Tel: 886 35731695. Fax: 886 35723764. E-mail: tmchen@mail.nctu.edu.tw.
† Phosphor Research Laboratory, National Chiao Tung University.
‡ Materials and Chemical Research Laboratories, Industrial Technology Research Institute.
§ Applied Solid-State Laboratory, National Chiao Tung University.
# National Synchrotron Radiation Research Center, Hsinchu Science Park.

(1) Justel, T.; Krupa, J. C.; Wiechert, D. U. *J. Lumin.* **2001**, *93*, 179.
(2) Koike, J.; Kojima, T.; Toyanaga, R.; Kagami, A.; Hase, T.; Inaho, H. *J. Electrochem. Soc.* **1979**, *126*, 1008.
(3) de Jager-Veenis, A. W.; Bril, A. *J. Electrochem. Soc.* **1976**, *123*, 1253.
(4) Okazaki, C.; Shiiki, M.; Suzuki, T.; Suzuki, K. *J. Lumin.* **2000**, *87*, 1280.
(5) Yokota, K.; Zhang, S. X.; Kimura, K.; Sakamoto, A. *J. Lumin.* **2001**, *92*, 223.
(6) Lu, S. W.; Copealand, T.; Lee, B. I.; Tong, W.; Wagner, B. K.; Park, W.; Zhang, F. *J. Phys. Chem. Solids* **2001**, *62*, 777.
(7) Shionoya, S.; Yen, W. M. *Phosphor Handbook*; CRC Press: Boca Raton, FL, 1999; p 190.
(8) Wang, Y.; Endo, T.; He, L.; Wu, *C. J. Cryst. Growth* **2004**, *268*, 568.
(9) Chakoumakos, B. C.; Arbraham, M.; Boatner, L. A. *J. Solid State Chem.* **1994**, *109*, 197.

10.1021/cm061042a CCC: $37.00
Published on Web 06/02/2007

Table 1. Crystallographic Data for YVO_4, YPO_4, $GdVO_4$, and $GdPO_4$

	YVO_4	YPO_4	$GdVO_4$	$GdPO_4$
cryst syst	zircon tetragonal	zircon tetragonal	zircon tetragonal	monoclinic
space group	I41/amd (no.141)	I41/amd (no.141)	I41/amd (no.141)	P121/n1(no.14)
a (Å)	7.1183(1)	6.8947(6)	7.2122(7)	6.6435(9)
b (Å)	7.1183(1)	6.8947(6)	7.2122(7)	6.8414(10)
c (Å)	6.2893(1)	6.0276(6)	6.346(2)	6.3281(6)
α (deg)	90	90	90	
β (deg)	90	90	90	103.98(1)
γ (deg)	90	90	90	
point-group symmetry	D_{4h}	D_{4h}	D_{4h}	P_2
coordination no.	Y(8); V(4); O(3)	Y(8); P(4); O(3)	Gd(8); V(4); O(3)	Gd(8); P(4); O(3)
refs	9	9, 22	24	23

become an important task for which research is being actively pursued.

The crystal structure of MVO_4 (M = Y, Ce, Pr, Nd, Tb, Ho, Er, Tm, Yb, Lu) of type zircon ($ZrSiO_4$) was refined with Rietveld analysis on the basis of neutron powder-diffraction data by Chakoumakos et al.;[9] these authors discovered that MVO_4 crystallizes in the tetragonal system and can be described with space group $I4_1/amd$ and $Z = 4$, in which M is noncentrosymmetrically coordinated by eight oxygen atoms. Chakoumakos et al. reported also that the V−O distance exhibits a small systematic decrease with decreasing size of the M atom.[9] As YVO_4:Eu is known as a typical red-emitting phosphor for which the host crystallizes in a tetragonal structure, Wang et al. described the growth and characterization of $Y(V_{0.9}P_{0.1})O_4$ crystals and confirmed that $Y(V_{0.9}P_{0.1})O_4$ belongs to a $ZrSiO_4$-type structure with space group $I4_1/amd$; its lattice parameters were determined to be $a = b = 7.089(4)$ Å and $c = 6.253(2)$ Å.[10] Rambabu et al. investigated the synthesis, spectral characterization, and influence of host matrix composition on the luminescence and ambient decay lifetime of $LnPO_4$:Eu (Ln = Y, La, Gd) phosphors under ultraviolet excitation.[11] Sohn et al. reported a search on the mixed compositional system of Eu^{3+}-doped $Y(As,Nb,P,V)O_4$ for improved red-emitting phosphors using a combinatorial method and discovered a phosphor with optimal composition $Y_{0.9}(P_{0.92}V_{0.03}Nb_{0.05})O_4:Eu^{3+}$ of which the luminescence efficiency and Commission International de I'Eclairage (CIE) color chromaticity at 147 nm excitation is comparable with that of the conventional $(Y,Gd)BO_3:Eu^{3+}$ phosphor.[12] Their results also indicated that the incorporation of V or Nb in a small proportion into the YPO_4 host matrix acts as a bridge for energy transfer, thereby enhancing the luminescence efficiency. They thus hinted that the route of energy transfer under VUV excitation was from the Y−O charge transfer (CT) to R−O CT in the RO_4^{3-} (R = V, Nb) anion group and then to the Eu^{3+} center.[12] These authors also reported that only $YPO_4:Eu^{3+}$, not $YVO_4:Eu^{3+}$, exhibits considerable emission upon VUV excitation. Minami et al. described the fabrication and investigated the luminescence properties of full-color thin films using $(Y_{1-x}Gd_x)VO_4$:R (R = Eu, Er, Tm) phosphors.[13] Zhang et al. reported a polyacrylamide gel synthesis at low temperature of nanocrystalline YVO_4:Eu, which exhibited greater luminescence intensity than bulk YVO_4:Eu.[14] To investigate the mechanism of luminescence and the role of Gd^{3+} in the energy transfer under VUV excitation, Wang et al. concluded that energy transfer occurs through the host lattice to Eu^{3+} via the overlap between the charge transfer of $Gd^{3+}-O^{2-}$ and the absorption of the BO_3^{3-} group in $(Y,Gd)BO_3$:Eu under excitation at 100−300 nm.[15] Yu et al. described the preparation of nanocrystalline $Y(V,P)O_4$:Eu and $RVO_4:Eu^{3+}$ thin films and found that YVO_4 and YPO_4 form a complete solid solution and that the *x* value in the $Y(P_{1-x}V_x)O_4:Eu^{3+}$ film has a great influence on the luminescence intensity, color, and decay behavior.[16]

To seek and develop satisfactory red-emitting PDP phosphors, we have thoroughly investigated the preparation and photoluminescence (PL) under VUV excitation of several modifications of Gd^{3+} and/or P^{5+}-co-doped $YVO_4:Eu^{3+}$-based phosphors and studied the spectral, optical, and chromaticity properties of the obtained phosphors. Here, we report the synthesis and VUV PL spectral investigations of red-emitting $(Y_{1-y-x}Gd_yEu_x)(V_{1-z}P_z)O_4$ phosphors in several series and investigated the dependence of luminescence performance on phosphor composition. On analysis of the VUV spectral and chromaticity investigations of these phosphors, we achieved an optimized composition for a new red-emitting phosphor with great potential for PDP application. The luminescence and chromaticity characteristics of $(Y_{1-x-y}Gd_y)(V_{1-z}P_z)O_4$:*x*Eu are compared against a commercial red-emitting phosphor $(Y,Gd)BO_3:Eu^{3+}$ as a reference. On the basis of these results, we evaluated the potential application of $(Y_{1-x-y}Eu_xGd_y)(V_{1-z}P_z)O_4$ as a red-emitting PDP phosphor.

2. Experimental Section

2.1. Materials and Synthesis. We prepared polycrystalline samples in two series with compositions $(Y_{1-x}Eu_x)(V_{1-z}P_z)O_4$ (abbreviated $Y(V_{1-z}P_z)O_4:xEu^{3+}$) and $(Y_{1-x-y}Eu_xGd_y)(V_{1-z}P_z)O_4$ (abbreviated $(Y_{1-y-x}Gd_y)(V_{1-z}P_z)O_4:x$Eu) through solid-state reactions. Briefly, the constituent oxides Y_2O_3 (99.99%), Gd_2O_3 (99.99%), Eu_2O_3 (99.99%), V_2O_5 (99.99%), and $(NH_4)_2HPO_4$ (99.99%) (all from Aldrich Chemicals, Milwaukee, WI) were intimately mixed in the requisite proportions. The mixtures were

(10) Wang, Y.; Lan, J.; Zhao, B.; Chen, J.; Lin, X.; Chen, J. *J. Cryst. Growth* **2004**, *263*, 296.
(11) (a) Rambabu, U.; Buddhudu, S. *Opt. Mater.* **2001**, *17*, 401. (b) Ropp, R. C. *J. Electrochem. Soc.* **1968**, *115*, 841.
(12) Sohn, K.-S.; Zeon, I. W.; Chang, H.; Lee, S. K.; Park, H. D. *Chem. Mater.* **2002**, *14*, 2140.
(13) Minami, T.; Miyata, T.; Suzuki, Y.; Mochizuki, Y. *Thin Solid Films* **2004**, *65*, 469.
(14) Zhang, H.; Fu, X.; Niu, X.; Sun, G.; Xin, Q. *J. Solid State Chem.* **2004**, *177*, 2649.
(15) Wang, Y.; Guo, X.; Endo, T.; Murakami, Y.; Ushirozawa, M. *J. Solid State Chem.* **2004**, *177*, 2242.
(16) Yu, M.; Lin, J.; Wang, S. B. *Appl. Phys. A* **2005**, *80*, 353.

calcined at 600 °C with 5 mass % H_3BO_3 added as a flux, reground, and sintered at four temperatures in a 1000−1300 °C range for 8 h to avoid possible incomplete reaction. The obtained product was then checked with X-ray diffraction (XRD) for impurity phases. A commercial PDP phosphor (Y,Gd)BO_3:Eu^{3+} (Kasei Optonix, Ltd., Kanagawa, Japan, catalog No. KX-504) served as a reference for comparison of VUV spectra and CIE chromaticity characteristics.

2.2. Material Characterizations. We verified the phase purity of the phosphor samples as prepared by powder X-ray diffraction (XRD) analysis with an advanced automatic diffractometer (Bruker AXS D8) with Cu K radiation ($\lambda = 1.5418$ Å) operating at 40 kV and 20 mA. The XRD profiles were collected in a range $10° < 2\theta < 80°$. Employing synchrotron radiation (SR) as a light source, we examined the excitation (PLE) and photoluminescence (PL) spectra excited with the vacuum ultraviolet (VUV) radiation. The VUV spectra were measured in part with a PDP phosphor-testing system (Zhejiang University Sensing Instruments Co., Ltd., China) equipped with VUV light sources (wavelengths 147 and 172 nm). For measurements with the synchrotron source, the intense and continuous VUV beam was dispersed from a cylindrical grating monochromator beam line coupled to the 1.5 GeV storage ring at the National Synchrotron Radiation Research Center in Taiwan; this beam line has four gratings, and its focal length is 6 m. We used the 450 grooves/mm grating that spans the wavelength range 100−350 nm. The emission from the phosphor was analyzed with a 0.32 m monochromator and detected with a photomultiplier in a photon-counting mode. We carefully normalized the incident excitation sources and measured the PL signals from phosphors of the same size; by this means, we quantitatively compared the normalized PL spectra for separate samples. The Commission International de I'Eclairage (CIE) chromaticity coordinates for all samples were measured with a color analyzer (Laiko model DT-100) equipped with a CCD detector (Laiko Co., Tokyo, Japan). Calculations of the electronic density of states were based on density-functional theory (DFT).

2.3. Band Structure Calculations. To understand the effect of charge transfer on the VUV luminescence intensity in (Y,Gd)(V,P)O_4:Eu^{3+} system, we used the full-potential linearized augmented-plane-wave (LAPW)[17−19] method to calculate the electronic structures of YPO_4, YVO_4, $GdPO_4$, and $GdVO_4$ with the program WIEN2K.[20] For $GdMO_4$ (M = P, V), the spin polarization calculations were performed. The exchange and correlation energies were treated within the density-functional theory (DFT), with a generalized gradient approximation (GGA) for the exchange and correlation potential within the Perdew−Burke−Ernzerhof model.[21] The truncation parameters for the basis set were $G_{max} = 14$ and $R_{mt} \times K_{max} = 7$; R_{mt} is the smallest radius of an atomic sphere in the unit cell and K_{max} is the magnitude of the largest k vector. The atomic radii/bohr (1 bohr = 0.529×10^{-10} m) values for Y, Gd, V, P, and O are 1.48, 1.4, 1.7, 1.38, and 1.44, respectively. The self-consistencies were carried out on 18, 6, and 10 k-points mesh in the irreducible Brillouin zone for tetragonal (YPO_4, YVO_4), spin

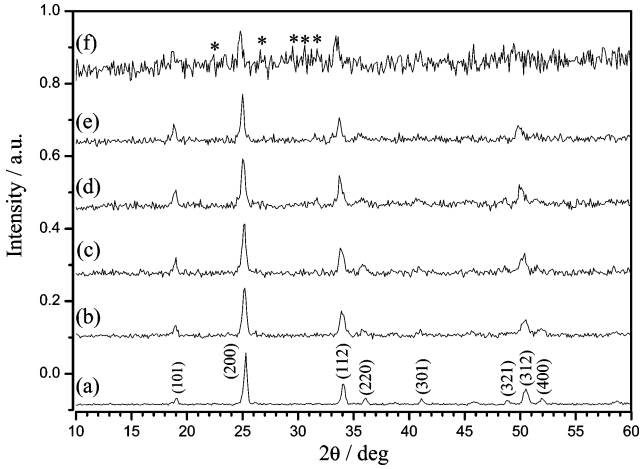

Figure 1. Comparison of XRD profiles of $(Y_{0.95-x}Gd_xEu_{0.05})(V_{0.6}P_{0.4})O_4$ with x = (a) 0, (b) 0.2, (c) 0.4, (d) 0.6, (e) 0.8, and (f) 0.95 (synthesized at 1200 °C; 8 h).

calculation of $GdVO_4$ and monoclinic $GdPO_4$, respectively. The self-consistencies were performed on 18 and 45 k-points mesh in the irreducible Brillouin zone for tetragonal (YPO_4, YVO_4, $GdVO_4$) and monoclinic ($GdPO_4$) structures. The gap between valence and core states is −6.0 Ry; convergence was assumed when the energy difference between cycles was less than 0.0001 Ry.

3. Results and Discussion

3.1. Phase Characterizations and XRD Analysis. As summarized in Table 1, the host matrices of YPO_4, YVO_4, and $GdVO_4$ crystallize in a tetragonal crystal system with space group $I4_1/amd$, whereas $GdPO_4$ crystallizes in a monoclinic system with space group $P2_1/n$ (No. 14). To investigate the composition optimization of potential red-emitting phosphovanadate-based phosphors for PDP applications, we have synthesized phosphors in several series with compositions $(Y_{1-x}Eu_x)(V_{1-z}P_z)O_4$, $(Y_{1-y}Gd_y)(V_{0.6}P_{0.4})O_4$:$Eu^{3+}$ and $(Y_{1-y}Gd_y)(V_{1-z}P_z)O_4$:$Eu^{3+}$. Moreover, all chemical compositions discussed in this work are nominal compositions.

A comparison of indexed XRD profiles for $(Y_{1-x}Eu_x)VO_4$ with x = 0, 0.01 0.03, 0.05, 0.07, and 0.09 (see the Supporting Information, Figure A) indicates that XRD patterns of Eu^{3+}-doped YVO_4 are consistent with that reported for YVO_4 (JCPDS 76-1649) and no shifting of diffraction features was observed with increasing proportion of doped Eu^{3+}; this observation is attributed to the similarity of ionic radii of Y^{3+} and Eu^{3+}. Furthermore, a series of indexed XRD profiles for $(Y_{0.95}Eu_{0.05})(V_{1-z}P_z)O_4$ with z = 0, 0.2, 0.4, 0.6, 0.8, and 1.0 (see the Supporting Information, Figure B) were found to agree satisfactorily with those reported for both YPO_4 (JCPDS 84-0335) and YVO_4 (JCPDS 76-1649). With the formation of a complete solid solution of $(Y_{0.95}Eu_{0.05})(V_{1-z}P_z)O_4$, we observed a systematic shifting of diffraction angle 2θ toward greater angle direction when z increases monotonically from 0 to 1.0. XRD profiles obtained from a series of $(Y_{0.95-y}Gd_yEu_{0.05})(V_{0.4}P_{0.6})O_4$ with y = 0, 0.2, 0.4, 0.6, 0.8, and 0.95 (synthesized at 1200 °C, 8 h) are summarized in Figure 1. Formation of only a partial solid solution between $Y(V_{0.6}P_{0.4})O_4$ and $Gd(V_{0.4}P_{0.6})O_4$ is expected, as YVO_4 (JCPDS 76-1649), $GdVO_4$ (JCPDS 17-

(17) Hohenberg, H.; Kohn, W. *Phys. Rev.* **1964**, *136*, B864.
(18) Kohn, W.; Sham, L. *Phys. Rev.* **1965**, *140*, A1133.
(19) Singh, D. *Planewaves, Pseudopotentials, and the LAPW Method*; Kluwer Academic: Boston, 1994.
(20) Blaha, P.; Schwarz, K.; Luitz, J. *WIEN97, A Full Potential Linearized Augmented Plane Wave Package for Calculating Crystal Properties*; Universität Wien: Vienna, Austria, 2000.
(21) Perdew, J. P.; Burke, K.; Ernzerhof, M. *Phys. Rev. Lett.* **1996**, *77*, 3865.
(22) Milligan W. O.; Mullica; D. F.; Beall, G. W.; Boatner, L. A. *Inorg. Chim. Acta* **1982**, *60*, 39.
(23) Mullica, D. F.; David A. Grossie; Boatner, L. A. *Inorg. Chim. Acta* **1985**, *109*, 105.
(24) Donald F. Mullica; Sappenfield, E. L.; Abraham, M. M.; Chakoumakos, B. C.; Boatner, L. A. *Inorg. Chim. Acta* **1996**, *248*, 85

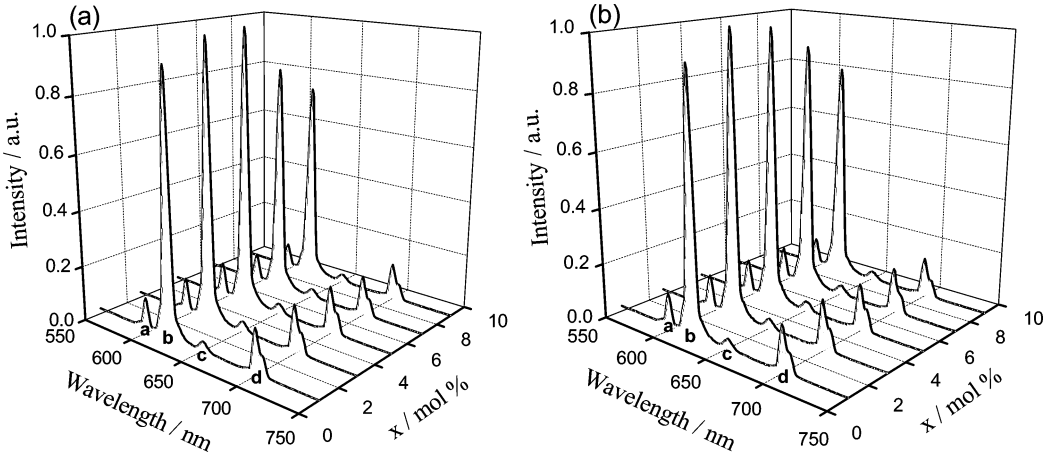

Figure 2. VUV PL spectra of $(Y_{1-x}Eu_x)VO_4$ (x = 1, 3, 5, 7, and 9%): λ_{ex} = (a) 147 and (b) 172 nm (a, $^5D_0 \rightarrow {}^7F_1$; b, $^5D_0 \rightarrow {}^7F_2$; c, $^5D_0 \rightarrow {}^7F_3$; d, $^5D_0 \rightarrow {}^7F_4$).

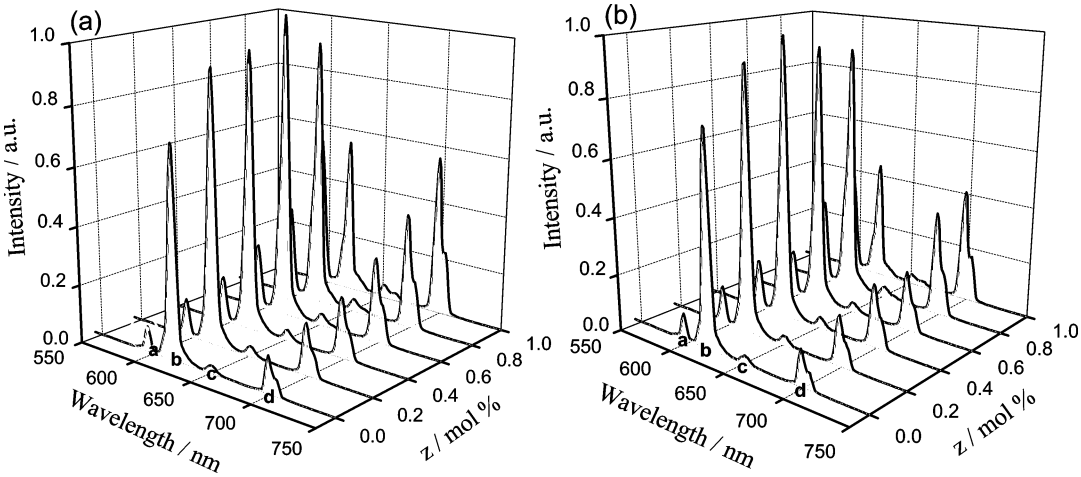

Figure 3. VUV PL spectra of $(Y_{0.95}Eu_{0.05})(V_{1-z}P_z)O_4$ (z = 0, 0.2, 0.4, 0.6, 0.8, 1.0): λ_{ex} = (a)147 and (b)172 nm (a, $^5D_0 \rightarrow {}^7F_1$; b, $^5D_0 \rightarrow {}^7F_2$; c, $^5D_0 \rightarrow {}^7F_3$; d, $^5D_0 \rightarrow {}^7F_4$).

0260), and $GdPO_4$ (JCPDS 32-0386) are known to crystallize in disparate structures, as indicated in Table 1. A careful analysis of Figure 1 revealed that the XRD patterns shown in Figures 1d−f cannot be completely indexed and become increasingly complicated with increasing content of doped Gd^{3+}. When all Y^{3+} ions are replaced by Gd^{3+} ions, the peaks that are indexed as $GdPO_4$ (32-0386) appear (marked by asterisk). The maximum proportion of Y to be replaced by Gd was hence estimated to be ca. 0.8.

We calculated the lattice parameters on the basis of the XRD patterns. In the tetragonal $(Y_{0.95}Eu_{0.05})(V_{1-z}P_z)O_4$ series with z = 0, 0.2, 0.4, 0.6, 0.8, and 1.0, lattice parameters a (= b) and c decreased with increasing content of P, which we rationalize according to the fact that the radius of P is smaller than that of V and that a solid solution is formed. On the other hand, when increasing the content of Gd^{3+} in $(Y_{0.95-y}Gd_yEu_{0.05})(V_{0.4}P_{0.6})O_4$ with y = 0, 0.2, 0.4, 0.6, 0.8, and 0.95. Both lattice parameters a (= b) and c increase when Y^{3+} is increasingly replaced with Gd^{3+}, which we rationalize according to the fact that the radius of Gd^{3+} is larger than that of Y^{3+}.

3.2. Analysis of VUV Spectra. Shown in panels a and b of Figure 3 are the VUV PL spectra of $(Y_{1-x}Eu_x)VO_4$ under excitation at 147 and 172 nm, respectively. As indicated in Figure 2, the emission maxima of PL spectra for $(Y_{1-x}Eu_x)VO_4$ phosphors are attributed to the multiplet transitions $^5D_0 \rightarrow {}^7F_J$ (J = 1, 2, 3, 4) of Eu^{3+}. In the absence of inversion symmetry at the Eu^{3+} (or Y^{3+}) lattice site, the electric-dipole transition would dominate. As a result, the intensity of electric-dipole allowed transitions $^5D_0 \rightarrow {}^7F_{2,4}$ was much stronger than that of magnetic-dipole allowed transitions $^5D_0 \rightarrow {}^7F_{1,3}$. As indicated by the VUV PL spectra shown in Figure 2, the emission spectra of $(Y_{1-x}Eu_x)VO_4$ (x = 0.01, 0.03, 0.05, 0.07, 0.09) are mainly dominated by $^5D_0 \rightarrow {}^7F_2$ regardless of the excitation wavelength. To optimize the activator content doped in the host lattice, we measured the emission intensity as a function of Eu^{3+} concentration relative to Y^{3+}. The intensity of transition $^5D_0 \rightarrow {}^7F_2$ was found to increase with increasing Eu^{3+} concentration. The content of doped Eu^{3+} was hence maintained at 5% for all phosphor samples discussed in the followings. The PL intensity was found to decrease for a concentration of doped Eu^{3+} greater than 5%, which is attributed to a concentration-quenching effect. When the wavelength of excitation was altered from 147 to 172 nm, as shown in Figure 2b, the VUV PL spectra resembled, in both shape and trend of the $I-\lambda$ curve, those obtained under excitation at 147 nm.

As the YPO_4 host is reported to show strong absorption in the VUV range,[12] we have attempted to design a PDP phosphor with great VUV efficiency by partly substituting

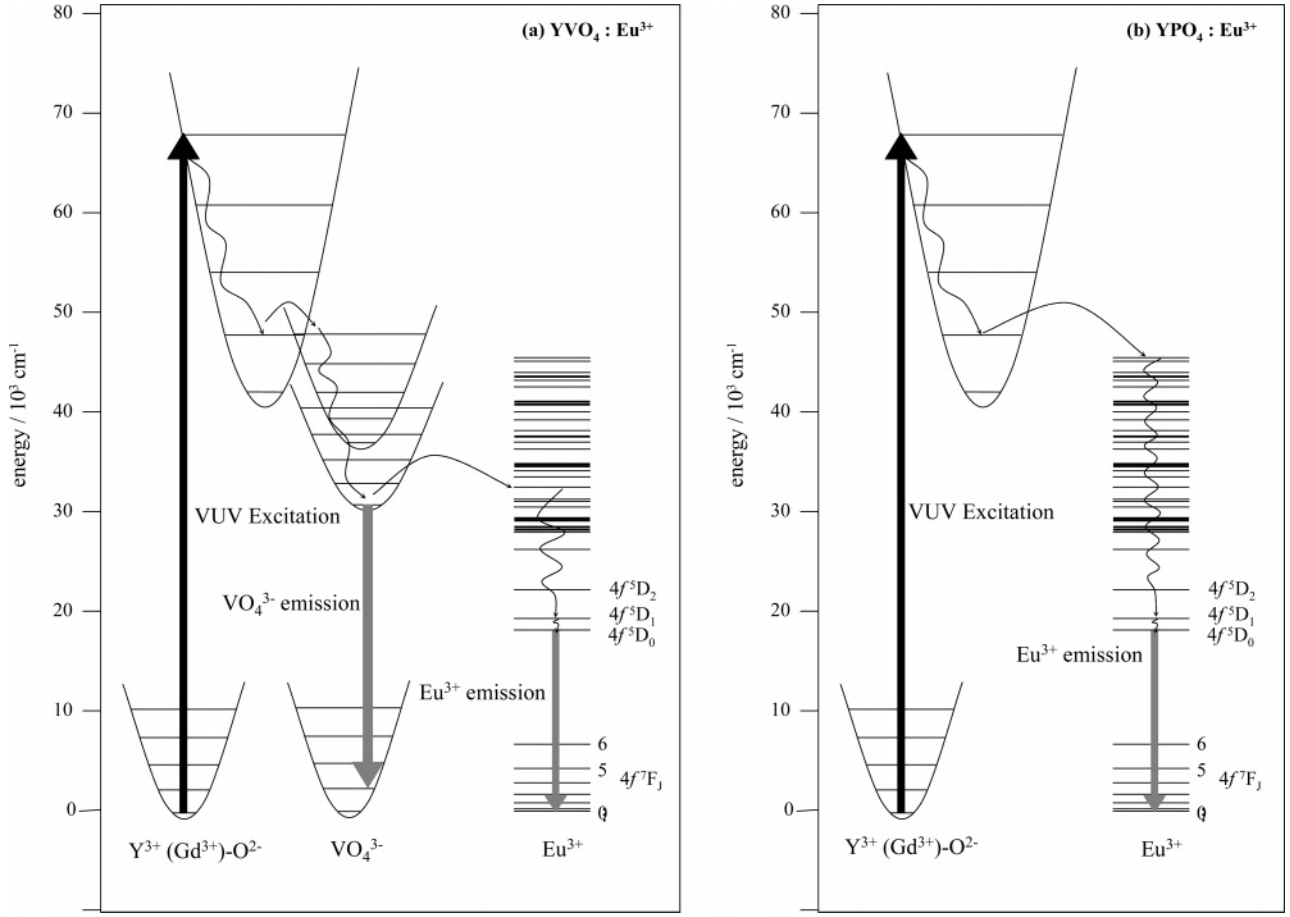

Figure 4. Part of the energy level scheme of (a) YVO_4:Eu and (b) YPO_4:Eu. Excitation, emission, and energy-transfer processes are indicated.

V^{5+} by isovalent P to form phosphors in a series with normal composition $(Y_{0.95}Eu_{0.05})(V_{1-z}P_z)O_4$. As indicated in Figure 3, the PL intensity of transition $^5D_0 \rightarrow {}^7F_2$ attributed to $(Y_{0.95}Eu_{0.05})(V_{1-z}P_z)O_4$ first increased with increasing z value and then attained a maximum for samples with $z = 0.6$ ($\lambda_{ex} = 147$ nm) and 0.4 ($\lambda_{ex} = 172$ nm), respectively. As a result, the doping concentration of P was maintained at 40 mol % for phosphors discussed in the following. Furthermore, the PL intensity attributed to Eu^{3+} in $(Y_{0.95}Eu_{0.05})(V_{1-z}P_z)O_4$ was discovered to decrease when the value of z exceeded the maximum point (i.e., $z = 0.6$; $\lambda_{ex} = 147$ nm).

As rationalized by Sohn et al.[12] for the red-emitting YVO_4:Eu^{3+}, upon VUV excitation, the energy is first absorbed by the host lattice YVO_4 through a charge-transfer mechanism, which involves a transition between a 4d-like state of Y atom and a 2p-like state of oxygen atom. The absorbed energy was then transferred to VO_4^{3-} groups, and eventually, to a Eu^{3+} luminescence center and then relaxed as $^5D_0 \rightarrow {}^7F_J$ emission. Instead of transferring energy to Eu^{3+}, the energy may be relaxed to the ground state of the VO_4^{3-} group directly. But the relaxation process is less efficient than the transition process in this case; the emission peak of VO_4^{3-} is hard to find. The whole process is illustrated in Figure 4a.[25] The same as that in YVO_4:Eu^{3+}, the route of energy transfer in YPO_4:Eu^{3+} involves energy absorption by charge-transfer mechanism involving $Y^{3+}-O^{2-}$. But the energy is directly transferred to the Eu^{3+} center without passing the PO_4^{3-} group, as indicated in Figure 4b.[25] As energy transfer in YPO_4 is inefficient, a VO_4^{3-} group is required to act as a bridge between the host absorption and the Eu^{3+} luminescence center by the $Y^{3+}-O^{2-}$ charge-transfer (CT) transition. For this reason, the PL intensity of transition $^5D_0 \rightarrow {}^7F_2$ was observed to decrease when P was doped at a sufficiently large proportion (i.e., $z > 0.4$) into the host lattice of $(Y_{0.95}Eu_{0.05})(V_{1-z}P_z)O_4$.

The relative intensity of $^5D_0 \rightarrow {}^7F_J$ multiplet emission is also an important factor that determines the chromaticity or saturation of red color; in general, the larger the magnitude of $(({}^5D_0 \rightarrow {}^7F_2)/({}^5D_0 \rightarrow {}^7F_1))$ (R/O), the closer to the optimal value of the color chromaticity. We also observed that the R/O ratio decreased with increasing z value or increasing P/V ratio, respectively. This observation can be rationalized by the fact that the energy of the CT attributed to $Eu^{3+}-O^{2-}$ in phosphate, is too great to make the parity-forbidden $4f-4f$ transitions of Eu^{3+} acquire intensity from a charge-transfer mechanism.[12]

Beyond investigating the partial substitution of V with P to improve the PL efficiency, we also tried to co-dope Gd^{3+} into the Y^{3+}-site of $(Y_{0.95}Eu_{0.05})(V_{0.4}P_{0.6})O_4$, of which the composition had been previously optimized, to form $(Y_{0.95-y}Gd_yEu_{0.05})(V_{0.4}P_{0.6})O_4$ phosphors in a series with varied y value. Through the structural similarity of $Y(V_{0.4}P_{0.6})O_4$:Eu and $(Y_{0.95-y}Gd_y)(V_{0.4}P_{0.6})O_4$:Eu, the VUV PL spectra

(25) Riwotzki, K.; Hasse, M. *J. Phys. Chem. B* **2001**, *105*,12709.
(26) Zeng, X.; Im, S.-J.; Jang, S.-H.; Kim, Y.-M.; Park, H.-B.; Son, S.-H.; Hatanaka, H.; Kim, G.-Y.; Kim, S.-G. *J. Lumin.*, **2006**, *121*,1.

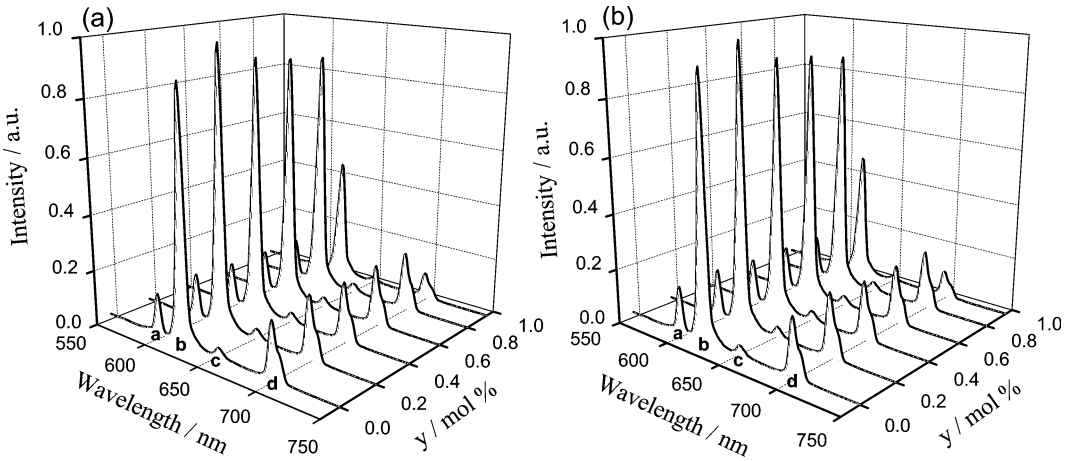

Figure 5. VUV PL spectra of $(Y_{0.95-y}Gd_yEu_{0.05})(V_{0.4}P_{0.6})O_4$ (y = 0, 0.2, 0.4, 0.6, 0.8, 0.95): λ_{ex} = (a)147 and (b)172 nm (a, $^5D_0 \rightarrow {}^7F_1$; b, $^5D_0 \rightarrow {}^7F_2$; c, $^5D_0 \rightarrow {}^7F_3$; d, $^5D_0 \rightarrow {}^7F_4$).

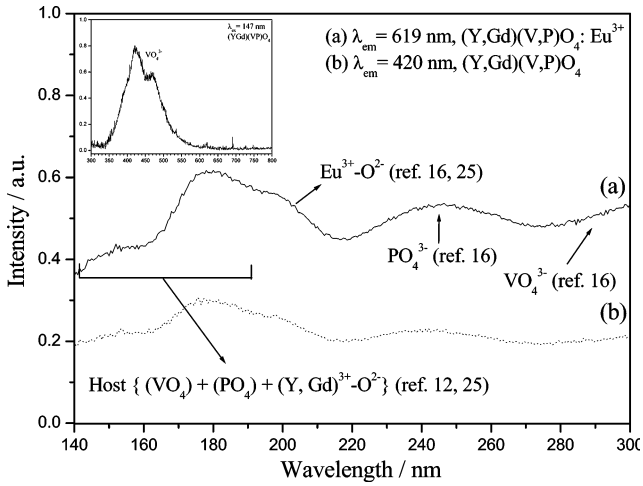

Figure 6. VUV PLE spectra of $(Y_{0.75}Gd_{0.2}Eu_{0.05})(V_{0.4}P_{0.6})O_4$ (solid line, monitored at λ_{em} = 619 nm), KX-504A (dashed line, monitored at λ_{em} = 592 nm), and $(Y_{0.8}Gd_{0.2})(V_{0.4}P_{0.6})O_4$ host (dotted line, monitored at λ_{em} = 420 nm). The inset indicates VUV PL spectra excited at 147 nm.

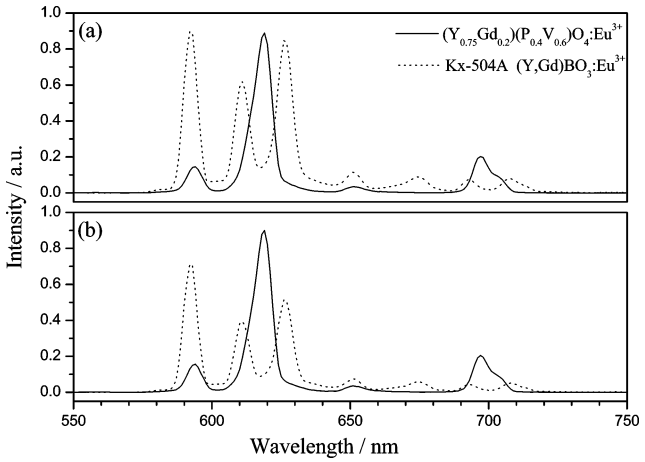

Figure 7. VUV PL spectra of $(Y_{0.75}Gd_{0.2}Eu_{0.05})(V_{0.4}P_{0.6})O_4$ (solid line), and commercial phosphors KX-504A (dash line): λ_{ex} = (a)147 and (b)172 nm.

have similar features except for the emission intensity. Shown in Figure 5 is the dependence of doped Gd^{3+} content on the PL intensity of $^5D_0 \rightarrow {}^7F_2$ emission observed for $(Y_{0.95-y}Gd_yEu_{0.05})(V_{0.4}P_{0.6})O_4$ phosphors with y = 0, 0.2, 0.4, 0.6, 0.8, 0.95, for which the PL intensity was observed to increase abruptly when Gd at a small proportion (i.e., y = 0.2) was doped into the host. As part of the absorption band of Gd^{3+} overlaps with the CT band from VO_4^{3-} to the Eu^{3+} center, the Gd^{3+}-doping produces more efficient excitation in the Eu^{3+} center when Gd^{3+} is co-doped,[8,16] but according to the results presented in Figure 5, concentration quenching is attributed to excessive doping of Gd^{3+} (i.e., y > 0.2) that gradually imposes a detrimental effect on the VUV PL intensity. The optimal dopant proportion of Gd^{3+} was thus selected as 0.2 to form a composition $(Y_{0.75}Gd_{0.20}Eu_{0.05})(V_{0.4}P_{0.6})O_4$ that was adopted for the following spectral and optical investigations.

To investigate the optical properties of $(Y_{0.75}Gd_{0.20})(V_{0.4}P_{0.6})O_4$:$Eu^{3+}$ with optimized composition, we measured the VUV PL and PLE spectra for both pristine and Eu^{3+}-activated $(Y_{0.8}Gd_{0.20})(V_{0.4}P_{0.6})O_4$ phosphors; the results appear in Figure 6. In the upper left inset of Figure 6, only a broad emission line spanning from 328 to 600 nm was observed, attributed to emission of the VO_4^{3-} group. When Eu^{3+} was doped into the host lattice to form $(Y_{0.75}Gd_{0.20})(V_{0.4}P_{0.6})O_4$:$Eu^{3+}$, only emission signals of Eu^{3+} were observed as indicated in Figure 5, which was attributed to energy transfer from the VO_4^{3-} group to the Eu^{3+} center, as already discussed above. The PLE spectra presented in Figure 6 were measured in the range 125−300 nm on monitoring the emissions attributed to transitions $^5D_0 \rightarrow {}^7F_2$ (Figure 6a) and VO_4^{3-} (Figure 6b). Charge-transfer transitions occur when a valence electron transfers from the ligand to unoccupied orbitals of the metal cation and are generally manifest through broad absorption or emission in the VUV−UV spectral region. To evaluate the performance and potential application of our phosphors, we measured and compared the PL spectra (Figure 7) of composition-optimized $(Y_{0.75}Gd_{0.20})(V_{0.4}P_{0.6})O_4$:$Eu^{3+}$ and a commercial red-emitting PDP phosphor KX-504A excited by vacuum ultraviolet radiation at 147 and 172 nm, respectively. As shown in plots a and b of Figure 6, a comparison of VUV PLE spectra for $(Y_{0.75}Gd_{0.20}Eu_{0.05})(V_{0.4}P_{0.6})O_4$ (monitored at λ_{em} = 619 nm) and $(Y_{0.8}Gd_{0.20})(V_{0.4}P_{0.6})O_4$ (monitored at λ_{em} = 420 nm) reveals that several CT absorption features attributed to PO_4^{3-}, VO_4^{3-}, and R^{3+}−O^{2-} (R = Y, Gd, Eu) have been identified. For instance, the band appearing in the region from 164 to 190 nm (plots a and b of Figure 6) is assigned to the CT transition between Y^{3+} and O^{2-}.[16] This observation hints that the excitation

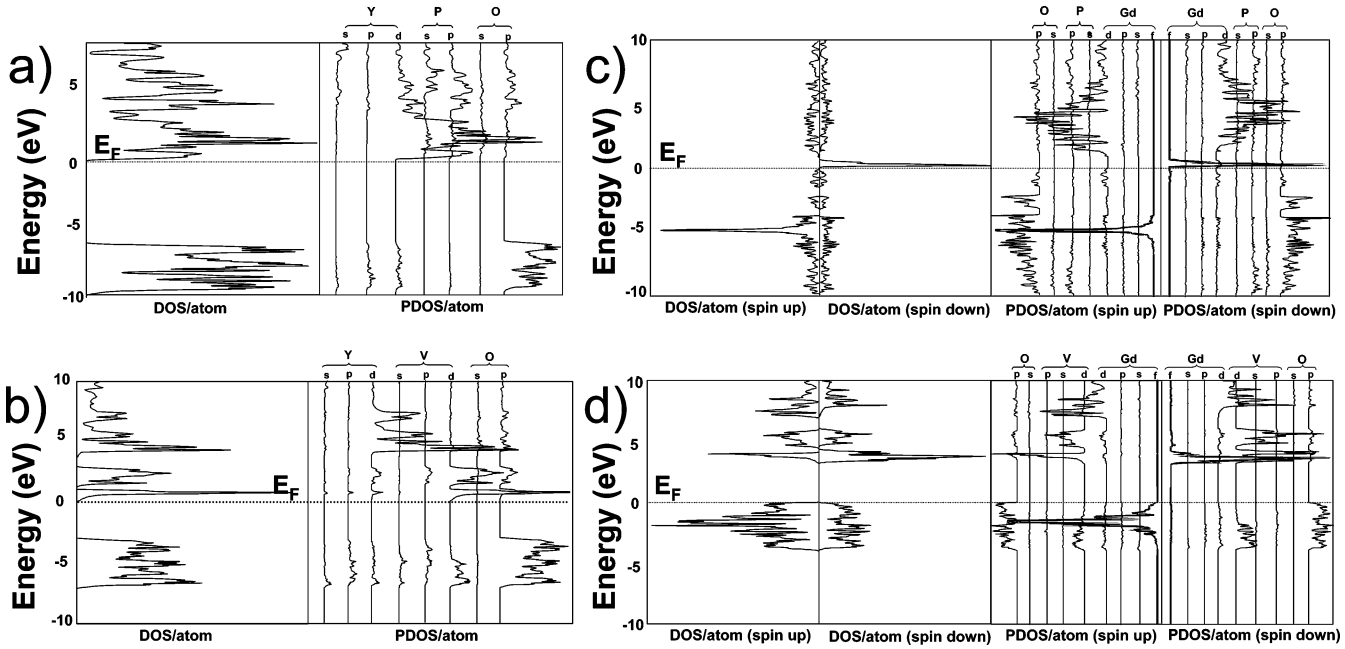

Figure 8. DOS curves of (a) YPO_4, (b) YVO_4, (c) $GdPO_4$, and (d) $GdVO_4$. The first column shows the total DOS; the Fermi energy is the zero of the energy scale.

energy is first absorbed by the host lattice involving the transition between 4d-like states of Y and 2p-like states of the oxygen atom. Then, the absorbed energy was transferred to the anionic RO_4^{3-} (R = V, P) group, as suggested by Wang et al.[16] We thus observed one band in the spectral region from 218 to 300 nm attributed to the CT transition from the oxygen atom to the central V^{5+} ion of the VO_4^{3-} anion.[13]

As indicated by PLE spectra shown in Figure 6, the absorption appearing at 178 nm is assigned to the $Gd^{3+}-O^{2-}$ CT transition that overlaps that attributed to the CT transition of $Eu^{3+}-O^{2-}$ at 196 nm, indicating that Eu^{3+} acquires energy from the $Gd^{3+}-O^{2-}$ energy transfer.[27] This observation explains why the observed PL intensity is significantly greater in $(Y_{0.95-y}Gd_yEu_{0.05})(V_{0.4}P_{0.6})O_4$ phases than those without Gd^{3+}-co-doping. In Figure 6, we also observed the CT transition of $Eu^{3+}-O^{2-}$ at 196 nm and an overlap between the CT transition bands of Gd^{3+}-O^{2-} and $Eu^{3+}-O^{2-}$. We also noted that the intensities of both the CT transition and the emission attributed to the transition $^5D_0 \rightarrow {}^7F_2$ under VUV excitation at 172 nm are greater than that at 147 nm. The PL intensity of $(Y_{0.75}Gd_{0.20}Eu_{0.05})$-$(V_{0.4}P_{0.6})O_4$ excited at 172 nm is much greater than that with excitation at 147 nm.

Furthermore, as indicated by a comparison of VUV PL spectra (Figure 7) measured at varied λ_{ex}, we observed that VUV absorption of $(Y_{0.75}Gd_{0.20}Eu_{0.05})$ $(V_{0.4}P_{0.6})O_4$ is much more intense than that of KX-504A. As indicated in Figure 7, under VUV excitation, the integrated peak area of our phosphor $(Y_{0.75}Gd_{0.20}Eu_{0.05})(V_{0.4}P_{0.6})O_4$ is 55% (i.e., excited at 147 nm) or 70% (i.e., excited at 172 nm) of that for KX-504A. These observations hint that $(Y_{0.75}Gd_{0.20}Eu_{0.05})(V_{0.4}P_{0.6})$-$O_4$ might serve as a promising substitute for KX-504A as a red-emitting PDP phosphor as future optimization of sample preparation is completed. Tests of luminous efficiency on phosphor powder and a PDP panel using our new phosphovanadate-based phosphors are currently in progress.

3.3. Results of Densities of States (DOS) Calculations. The band calculations at the DFT level were employed to calculate the electronic structure of RMO_4 (R = Y, Gd; M = P, V) and understand its physical properties and interatomic interactions. Figure 8 shows the total density of states (DOS) and the projected DOS curves for (a) YPO_4, (b) YVO_4, (c) $GdPO_4$, and (d) $GdVO_4$, respectively. The DOS curve of YPO_4 shows that the contributions of electronic states near the valence (VB) and conduction bands (CB) are dominated by the O(2p) and Y(4d) orbitals. The two features between −15 and −10 eV consists mainly of the P−O bonding states from P(3s, 3p) and O (2p) orbitals. The results indicate that charge transfers from O(2p) to Y(4d) orbitals. The DOS curve of YVO_4 show varied orbital contributions near the Fermi level (E_F) compared to YPO_4. As the V(3d) orbital is located between Y(4d) and O(2p), orbital interactions in these orbitals yield significant contributions of the Y band in VB and CB. These results show that the valence band about −10 to 0 eV consists mainly of O(2p), V(4s and 3d), and Y(4d) states that correspond to V−O and Y−O bonding interactions. The orbital contribution of YVO_4 above E_F is composed of V(3d, major), Y(4d, minor), and O(2p, minor) orbitals. The calculated electronic structure indicates that the charge transfer might occur not only in O(2p)−V(3d) but also in O(2p)−Y(4d). The transition metal hence plays a important role in improving the electron-transfer efficiently to a rare-earth atom, consistent with the enhancement of the optical transition in V-doped phases of the $(Y,Gd)(V,P)O_4$:Eu^{3+} system. For $GdPO_4$, the density of states about E_F are dominated by the O(2p), Gd(5d) orbitals, and a sharp feature at the Fermi level is contributed by localized Gd(4f) orbitals. The 4f states contain occupied 4f peaks (spin down) and unoccupied 4f peaks (spin up) separated by ca. 5 eV. There

(27) Sato, Y.; Kumagai, T.; Okamoto, S.; Yamamoto, H.; Kunimoto, T. *Jpn. J. Appl. Phys.* **2004**, *43*, 3456.

Table 2. Comparison of CIE Chromaticity Coordinates of Phosphors (λ_{ex} = 172 nm)

phosphors	*x*	*y*	phosphors	*x*	*y*
$(Y_{0.99}Eu_{0.01})VO_4$	0.6675	0.3270	$(Y_{0.95}Eu_{0.05})(V_{0.6}P_{0.4})O_4$	0.6651	0.3295
$(Y_{0.97}Eu_{0.03})VO_4$	0.6705	0.3275	$(Y_{0.75}Gd_{0.2}Eu_{0.05})(V_{0.6}P_{0.4})O_4$	0.6614	0.3286
$(Y_{0.95}Eu_{0.05})VO_4$	0.6718	0.3275	$(Y_{0.55}Gd_{0.4}Eu_{0.05})(V_{0.6}P_{0.4})O_4$	0.6608	0.3286
$(Y_{0.93}Eu_{0.07})VO_4$	0.6735	0.3269	$(Y_{0.35}Gd_{0.6}Eu_{0.05})(V_{0.6}P_{0.4})O_4$	0.6599	0.3282
$(Y_{0.91}Eu_{0.09})VO_4$	0.6748	0.3262	$(Y_{0.15}Gd_{0.8}Eu_{0.05})(V_{0.6}P_{0.4})O_4$	0.6524	0.3262
			$(Gd_{0.95}Eu_{0.05})(V_{0.6}P_{0.4})O_4$	0.6338	0.3229
$(Y_{0.95}Eu_{0.05})VO_4$	0.6718	0.3275			
$(Y_{0.95}Eu_{0.05})(V_{0.8}P_{0.2})O_4$	0.6691	0.3283			
$(Y_{0.95}Eu_{0.05})(V_{0.6}P_{0.4})O_4$	0.6651	0.3295			
$(Y_{0.95}Eu_{0.05})(V_{0.4}P_{0.6})O_4$	0.6572	0.3311			
$(Y_{0.95}Eu_{0.05})PO_4$	0.5946	0.3393			

is little, if any, contribution of Gd(5d) orbitals to the VB, indicating that the bonding interaction between Gd and O to be essentially ionic. These results indicate that charge transfer in this phase is mostly from O(2p) to Gd(5d) orbitals but internal charge transfer from Gd(4f) to Gd(5d) might occur. The DOS plot of $GdVO_4$ is essentially similar to that of YVO_4 except for an additional Gd(4f) orbital at the Fermi level. Most contributions about the Fermi level are from O(2p), V(3p, 3d), and Gd(5d) orbitals, indicating the bonding interactions of Gd−O and V−O bonds. The 4f states are made up of two peaks for spin down (occupied) and spin up (unoccupied) levels, which are separated by ca. 4 eV. The calculations suggest that the contribution of the filled Gd-(4f) states is close to the Fermi level, which may enhance the charge-transfer routes in O(2p)−V(3d) and O(2p)−Gd-(5d), and f−d excitation. Our results are in consistent with the observation that doping Gd^{3+} into the (Y,Gd)(V,P)O_4:Eu^{3+} system enhances the VUV luminescence intensity.

3.4 Investigations of Chromaticity Characteristics. For practical applications, in addition to luminescence efficiency and brightness, the color chromaticity is considered to be a critical parameter for evaluation of the performance of PDP phosphors. The CIE color coordinates (*x*,*y*) of all phosphors investigated in this work are compared in Table 2. For $(Y_{1-x}Eu_x)VO_4$ phosphors in a series with varied Eu^{3+}-dopant content, the CIE (*x*,*y*) values were independent of the dopant concentration. Moreover, for $(Y_{0.95}Eu_{0.05})(V_{1-z}P_z)O_4$ phosphors in a second series with varied content of P, our analysis of (*x*,*y*) values indicates that *x* decreases as the concentration of P dopant increases, whereas *y* increases, and the chromaticity shifts from pure red toward orange-red. As for co-doping of Gd^{3+}, both *x* and *y* decreased with increasing concentration of doped Gd^{3+}, but the range of shift upon Gd^{3+}-doping is too small and can be ignored. To understand the dependence of chromaticity on the composition of dopant P, we investigated the evolution of CIE chromaticity coordinates for $(Y_{0.95}Eu_{0.05})(V_{1-z}P_z)O_4$ (z = 0, 0.2, 0.4, 0.6, 1.0) as a function of *z*; the results are also summarized in Table 2. With increasing *z* (from right to left), the *x*-coordinate measured for $(Y_{0.95}Eu_{0.05})(V_{0.4}P_{0.6})O_4$ decreased from 0.6719 (z = 0) to 0.5946 (z = 1.0) with the *y*-coordinate remaining almost constant, indicating worse color saturation in the red. The systematic evolution of the chromaticity coordinate is considered to be related to the stronger VUV absorption of YPO_4 than that of YVO_4 as discussed previously.[13] These results show that our phosphors exhibit superior color saturation. The experimental chromaticity coordinates of red-emitting composition-optimized $(Y_{0.75}Gd_{0.20}Eu_{0.05})(V_{0.4}P_{0.6})O_4$ were studied against those for KX-504A as a reference, and the color purity of $(Y_{0.75}Gd_{0.20}Eu_{0.05})(V_{0.4}P_{0.6})O_4$ is greater in the red than that of commercial phosphor KX-504A.

4. Conclusions

We have prepared several series of red-emitting (Y,Gd)-(V,P)O_4:Eu^{3+} phosphors via a high-temperature, solid-state route and investigated the synthesis, microstructure, and luminescence properties of the red-emitting phosphors under VUV excitation. We measured the VUV PL and PLE spectra and chromaticity characteristics for the synthesized phosphors, and compared them with those of a commercial red-emitting phosphor. Our research shows that using the 172 nm wavelength is more efficient than the 147 nm one in pumping (Y,Gd)(V,P)O_4:Eu^{3+} phosphors. The composition of the new phosphor is optimized as $(Y_{0.75}Gd_{0.20}Eu_{0.05})(V_{0.4}P_{0.6})O_4$ and (Y,Gd)(V,P)O_4:Eu^{3+} can hence serve as an alternative phosphor to replace the widely used red-emitting (Y,Gd)BO_3:Eu^{3+} or Y_2O_3:Eu^{3+} commercial phosphors.

Acknowledgment. We appreciate generous financial support from the National Science Council of Taiwan, R.O.C., under Contracts NSC94-2113-M-009-001 and NSC95-2113-M-009-024-MY3 and thank the members of Dr. B.-M. Cheng's group at NSRRC, Taiwan, for providing facilities and assistance with VUV spectra measurements.

Supporting Information Available: Figures A and B (XRD profiles) in PDF format. This material is available free of charge via the Internet at http://pubs.acs.org.

CM061042A